Magnetic properties of X–Pt (X = Fe,Co,Ni) alloy systems

2004 J. Phys.: Condens. Matter 16 2317

(http://iopscience.iop.org/0953-8984/16/13/012)

INSTITUTE OF PHYSICS PUBLISHING JOURNAL OF PHYSICS: CONDENSED MATTER

J. Phys.: Condens. Matter **16** (2004) 2317–2334 PII: S0953-8984(04)73025-8

Magnetic properties of X–Pt (X = Fe, Co, Ni) alloy systems

Durga Paudyal, Tanusri Saha-Dasgupta and Abhijit Mookerjee

S N Bose National Centre for Basic Sciences, JD Block, Sector 3, Salt Lake City, Kolkata 700098, India

E-mail: dpaudyal@bose.res.in, tanusri@bose.res.in and abhijit@bose.res.in

Received 5 December 2003
Published 19 March 2004
Online at stacks.iop.org/JPhysCM/16/2317 (DOI: 10.1088/0953-8984/16/13/012)

Abstract

We have studied the electronic and magnetic properties of Fe–Pt, Co–Pt and Ni–Pt alloy systems in ordered and disordered phases. The influence of various exchange–correlation functionals on the values of equilibrium lattice parameters and magnetic moments in ordered Fe–Pt, Co–Pt and Ni–Pt alloys have been studied using the linearized muffin-tin orbital method. The electronic structure calculations for the disordered alloys have been carried out using an augmented space recursion technique in the framework of the tight binding linearized muffin-tin orbital method. The effect of short-range order has also been studied in the disordered phase of these systems. The results show good agreement with available experimental values.

1. Introduction

The magnetic and chemical interactions in solid solutions, their interdependence and the role they play in determining the electronic and magnetic properties of transition metal alloys have been the subject of extensive research for many years. The interplay between magnetism and spatial order in transition metal alloy systems has been extensively studied both experimentally [1–5] and using phenomenological models based on statistical thermodynamics [6–22].

In this paper, we studied the electronic and magnetic properties of ordered as well as disordered phase of the Fe–Pt, Co–Pt and Ni–Pt. Many studies on optical and magneto-optical characterization of these systems are available in the recent literature [23]. Nevertheless, a systematic first-principles study bringing out the interdependence of the magnetic and chemical ordering and the trend in this alloy series is lacking. The present paper aims at a systematic and comparative first-principles study of the electronic structure and magnetism in these systems, using techniques based on the local spin density approximation (LSDA) of the density functional theory.

Considering the case of ordered alloys, we have carried out a thorough study including careful investigation of the influence of various local, as well as non-local, exchange–correlation functionals on the value of the equilibrium lattice parameters and magnetic moments of ordered Fe–Pt, Co–Pt and Ni–Pt alloy systems.

The calculational scheme used for our calculations of disordered alloys is based on an augmented space recursion (ASR) technique. While the majority of the existing electronic structure calculations on *disordered* alloys have been based on the coherent potential approximation (CPA), the CPA, being a single-site mean-field approximation, cannot take into account the effect, at a site, of its immediate environment. As an alternative approach, Saha *et al* [24] have introduced the augmented space recursion (ASR) based on the combination of the augmented space formalism (ASF) first suggested by Mookerjee [25] and the recursion method of Haydock *et al* [26]. In this formalism, the configuration averaging is carried out without having to resort to single-site approximations. The recursion method allows one to take into account the effect of the local environment on electronic properties. Moreover, the convergence of various physical quantities calculated through recursion with the number of recursion steps and subsequent termination has been studied in great detail [27, 28]. Among the various advantages of the ASR in going beyond the single-site approximation is the possibility of the inclusion of local lattice distortions [29], which is important in the case of alloys with a size mismatch between components, as in the case of Fe–Pt, Co–Pt and Ni–Pt.

An important aspect in understanding the interplay between magnetism and ordering in disordered transition metal alloys involves investigation of the influence of the local environment, namely the short-range ordering (SRO) effect, on the electronic and magnetic properties of these alloys. There have been determinations of SRO parameters for different degrees of disorder using first-principles techniques [30–32] or extraction of these parameters from experiments and analysis of their effect on electronic structure and properties [33–35]. SRO for a disordered binary alloy A_xB_{1-x} is described, for example, by the Warren–Cowley parameter [36] which is defined as

$$\alpha_r^{AB} = 1 - \frac{P_r^{AB}}{y} \tag{1}$$

with the B atom occupying the rth nearest-neighbour site of the central A atom. $y = 1 - x$ denotes the macroscopic concentration of species B and P_r^{AB} is the joint probability of finding a B atom anywhere in the rth shell.

Mookerjee and Prasad [37] introduced a method for calculating the electronic structure of disordered alloys with short-range order (SRO) which is based on a generalization of the augmented space theorem [25]. Saha *et al* [38] implemented this within the framework of the recursion method. Later Ghosh *et al* [39] extended the technique to magnetic Co–Pt and Co-Pd systems. In the present paper we have carried out charge-self-consistent calculations based on this generalized ASR technique to examine the short-range ordering effect in Fe–Pt, Co–Pt and Ni–Pt systems.

This paper has been organized in the following manner. Section 2 is devoted to theoretical and computational details. The results of our study along with comparisons with existing experimental and theoretical studies have been discussed in section 3. We end the paper with the summary and conclusion in section 4. Some of the relevant equations of the generalized augmented space recursion method have been put in the appendix.

2. Theoretical and computational details

For ordered structures we have performed total energy density functional calculations. The Kohn–Sham equations were solved in the local spin density approximation (LSDA) with

von Barth–Hedin (vBH) [40] and Vosko–Wilk–Nusair (VWN) [41] exchange correlations as well as in the non-local (generalized gradient approximation (GGA)) Langreth–Mehl–Hu (LMH) [42] and Perdew–Wang (PW) exchange [43] correlations. The calculations have been performed in the basis of tight binding linear muffin-tin orbitals in the atomic sphere approximation (TB-LMTO-ASA) [44–47] including combined corrections. The calculations are semi-relativistic through the inclusion of mass-velocity and Darwin correction terms. The k-space integration was carried out with a $32 \times 32 \times 32$ mesh resulting in 969 k points for cubic primitive structures and 2601 k points for tetragonal primitive structures in the irreducible part of the corresponding Brillouin zone. The convergence of the magnetic moments with respect to k points has been checked. To get theoretical estimates of the equilibrium lattice parameters, we have carried out the minimization of the self-consistent TB-LMTO-ASA total energies, varying lattice parameters for Fe–Pt, Co–Pt and Ni–Pt alloys at different concentrations.

Our disordered calculations are based on the generalized ASR technique [37–39, 48, 49]. The Hamiltonian in the TB-LMTO minimal basis is sparse and therefore suitable for the application of the recursion method introduced by Haydock *et al* [26]. The ASR allows us to calculate the configuration averaged Green functions. It does so by augmenting the Hilbert space spanned by the TB-LMTO basis by the configuration space of the random Hamiltonian parameters. The configuration average is expressed *exactly* as a matrix element in the augmented space. A generalized form of this methodology is capable of taking into account the effect of short-range order (please see the appendix for the relevant equations). The initial guess TB-LMTO potential parameters for the self-consistency iterations for disordered alloy calculations are taken to be the potential parameters of the pure constituents. In subsequent iterations the potential parameters are obtained from the solution of the Kohn–Sham equation:

$$\left\{-\frac{\hbar^2}{2m}\nabla^2 + V^{\nu\sigma} - E\right\}\phi^{\nu}_{\sigma}(r_R, E) = 0 \tag{2}$$

where

$$V^{\lambda\sigma}(r_R) = V^{\lambda\sigma}_{\text{core}}(r_R) + V^{\lambda\sigma}_{\text{har}}(r_R) + V^{\lambda\sigma}_{xc}(r_R) + V_{\text{mad}}. \tag{3}$$

The electronic position within the atomic sphere centred at R is given by $r_R = r - R$. σ is the spin component. The core potentials are obtained from atomic calculations and are available for most atoms. For the treatment of the Madelung potential, we follow the procedure suggested by Kudrnovský *et al* [50] and use an extension of the procedure proposed by Andersen *et al* [44]. We choose the atomic sphere radii of the components in such a way that they preserve the total volume on average and the individual atomic spheres are almost charge neutral. This ensures that total charge is conserved, but each atomic sphere carries no excess charge. In doing so, one needs to be careful about the sphere overlap which should be under certain limits so as not to violate the atomic sphere approximation.

In these calculations one also needs to be very careful about the convergence of Fermi energy as well as that of magnetic moments. In fact, errors can arise in the augmented space recursion because one can carry out only a finite number of recursion steps and then terminate the continued fraction using available terminators. Also one chooses a large but finite part of the augmented space nearest-neighbour map and ignores that part of the augmented space very far from the starting state. This is also a source of error.

The formulation of the augmented space recursion as described in the appendix and used for calculation in the present paper is the energy-dependent augmented space recursion in which the disordered Hamiltonian with diagonal as well as off-diagonal disorder is recast into an energy-dependent Hamiltonian having only diagonal disorder. We have chosen a few seed points uniformly across the energy spectrum, carried out recursion on those points and spline

Table 1. The equilibrium lattice parameters in au of Fe–Pt, Co–Pt and Ni–Pt systems in ordered structures with various choices of exchange–correlation functionals. See the text for various abbreviations.

x	vBH	VWN	LMH	PW	Expt.
			$Fe_{1-x}Pt_x$		
0.00 (BCC)	5.28	5.30	5.36	5.54	5.406 [53]
(FCC)	6.47	6.47	6.53	6.63	6.877 [53]
0.25 ($L1_2$)	6.71	6.91	6.99	7.21	7.049 [54]
0.50 ($L1_0$)	$a = 7.16$	$a = 7.18$	$a = 7.22$	$a = 7.46$	$a = 7.253$ [53]
	$c = 6.94$	$c = 6.94$	$c = 7.02$	$c = 7.26$	$c = 7.020$ [53]
0.75 ($L1_2$)	7.25	7.27	7.30	7.54	7.313 [55]
			$Co_{1-x}Pt_x$		
0.00 (hex)	$a = 4.65$	$a = 4.66$	$a = 4.70$	4.83	4.728 [53]
	$c = 7.48$	$c = 7.49$	$c = 7.59$	7.78	7.675 [53]
(FCC)	6.55	6.56	6.63	6.81	6.684 [53]
0.25 ($L1_2$)	6.78	6.80	6.86	7.06	6.923 [54]
0.50 ($L1_0$)	$a = 7.14$	$a = 7.14$	$a = 7.18$	$a = 7.40$	$a = 7.204$ [53]
	$c = 6.78$	$c = 6.78$	$c = 6.86$	$c = 7.08$	$c = 7.007$ [53]
0.75 ($L1_2$)	7.21	7.22	7.25	7.50	7.240 [53]
			$Ni_{1-x}Pt_x$		
0.00 (FCC)	6.54	6.55	6.61	6.80	6.646 [53]
0.25 ($L1_2$)	6.77	6.78	6.84	7.05	6.890 [56]
0.50 ($L1_0$)	$a = 7.16$	$a = 7.16$	$a = 7.18$	$a = 7.42$	$a = 7.209$ [53]
	$c = 6.63$	$c = 6.64$	$c = 6.74$	$c = 6.96$	$c = 6.769$ [53]
0.75 ($L1_2$)	7.20	7.21	7.24	7.49	7.251 [56]
1.00 (FCC)	7.37	7.38	7.40	7.66	7.400 [53]

fit the coefficients of recursion throughout the whole spectrum. This enabled us to carry out a large number of recursion steps since the configuration space grows significantly less faster for diagonal, as compared with off-diagonal, disorder. The convergence of physical quantities with recursion steps has been discussed in detail earlier by Ghosh *et al* [51, 52].

We have checked the convergence of Fermi energy and magnetic moments with respect to recursion steps and the number of seed energy points for the case of the $NiPt_3$ system. We have found that the Fermi energy and magnetic moments converge beyond 7 recursion steps and 35 seed energy points. All our calculations reported in the following have been carried out with 8 recursion steps and 35 seed energy points.

3. Results and discussions

3.1. Lattice parameters

In table 1, we quote the values of equilibrium lattice parameters, obtained by minimizing the total energy with respect to the lattice parameters for $L1_2$ super-structures at 25 and 75% and a $L1_0$ super-structure at 50% concentration of Pt in Fe–Pt, Co–Pt and Ni–Pt alloy systems with different choices of local as well as non-local exchange–correlation potentials. The first comment is that non-local exchange–correlation potentials seem to decrease overbinding and predict larger equilibrium lattice parameters than the local ones. The PW seems to go overboard and give estimates of the equilibrium lattice parameters which are *larger* than the experimental values. The best agreement with experiment is found to be LMH.

Table 2. The local and average magnetic moments of the Fe–Pt system in ordered structures with various choices of exchange correlation functionals.

		Magnetic moment (μ_B/atom) of					
		With eq. lat. par.			With expt. lat. par.		
Concentration of Pt	XC used/expt. ref.	Fe	Pt	Average	Fe	Pt	Average
0.00 (BCC)	vBH (this work)	2.15			2.25		
	VWN (this work)	2.21			2.30		
	LMH (this work)	2.29			2.33		
	PW (this work)	2.55			2.35		
	Expt. [57]				2.22		
0.25 ($L1_2$)	vBH (this work)	0.00	0.00	0.00	2.57	0.32	2.01
	VWN (this work)	2.46	0.29	1.92	2.64	0.34	2.06
	LMH (this work)	2.63	0.33	2.06	2.70	0.35	2.11
	PW (this work)	2.78	0.35	2.17	2.68	0.37	2.10
	Auluck *et al* (vBH) [54]				2.56	0.26	1.99
	Podgorny (VWN) [55]	2.51	0.26	1.95			
	Hasegawa [16]				2.50	0.50	2.0
	Expt. [54]				2.70	0.50	2.15
0.50 ($L1_0$)	vBH (this work)	2.73	0.35	1.54	2.81	0.35	1.58
	VWN (this work)	2.79	0.35	1.57	2.85	0.35	1.60
	LMH (this work)	2.88	0.35	1.61	2.90	0.35	1.63
	PW (this work)	3.01	0.36	1.69	2.86	0.36	1.61
	Osterloh *et al* [58]				2.92	0.38	
	Podgorny (VWN) [55]	2.85	0.30	1.57			
	Expt. [58]				2.80		0.77
	Ferromagnetic calculation						
	vBH (this work)	2.99	0.31	0.98	3.10	0.32	1.02
	VWN (this work)	3.12	0.32	1.02	3.15	0.33	1.03
	LMH (this work)	3.19	0.34	1.05	3.20	0.34	1.06
	PW (this work)	3.24	0.39	1.11	3.12	0.37	1.06
	Podgorny [55]	3.22	0.34	1.06			
0.75 ($L1_2$)	Tohyama *et al* [59]				4.21	0.33	
	Anti-ferromagnetic calculation						
	vBH (this work)	3.11	0.15		3.16	0.15	
	VWN (this work)	3.17	0.15		3.20	0.15	
	LMH (this work)	3.24	0.15		3.25	0.16	
	PW (this work)	3.31	0.17		3.18	0.16	
	Podgorny [55]	3.46	0.16				
	Tohyama *et al* [59]				4.13	0.00	
	Expt. [60]				3.3		

3.2. Magnetism of Fe–Pt alloys

3.2.1. Ordered alloys. In table 2, we show two sets of calculations for magnetic moments in ordered Fe–Pt alloys. In the first set of calculations, we have calculated local as well as average magnetic moments corresponding to the theoretically estimated lattice parameters obtained via the energy minimization procedure. In the second set, calculations were done using experimental lattice parameters.

For a Fe_3Pt alloy in a $L1_2$ super-structure the use of the non-local exchange–correlation functionals LMH appears to give better agreement with experimental values [54] for local and average magnetic moments compared to local exchange–correlation functionals. This holds good for both choices of lattice parameters. The results for average and local magnetic moments from previous works by Auluck *et al* [54] and Podgorny [55], both using TB-LMTO, are in agreement with our corresponding results as can be seen from table 2. The differences seen with these results are primarily due to different computational details. Auluck *et al* [54] and Podgorny [55] have used the frozen core approximation in their calculations without taking into account f states for Pt. Podgorny and Auluck *et al* in their calculations used 286 and 84 k points in the irreducible part of the Brillouin zone (BZ), respectively. On the other hand, our calculations are all electron calculations taking a spdf minimal basis for Pt and using 969 k points in the irreducible part of the BZ. The local magnetic moment on Pt sites obtained by Hasegawa *et al* [16] using the augmented plane wave (APW) method is in exact agreement with the corresponding experimental value though their average magnetic moment and local magnetic moment on Fe sites are lower (by 0.20 μ_B for the average and 0.15 μ_B for Fe sites) than the corresponding experimental estimates [54]. Our calculation using the vBH functional for the exchange–correlation potential and theoretically estimated lattice parameter, leads to the conclusion of a non-magnetic ground state which is in agreement with that found in a previous study by Kubler *et al* [61]. This once again emphasizes that magnetic moments are very sensitively dependent on the particular exchange–correlation functional used and the detailed accuracy of the numerical calculations.

For FePt alloys the local magnetic moment of the Fe site in $L1_0$ super-structure calculated using the vBH exchange–correlation potential and experimental lattice parameter shows close agreement with the experimental value [58]. The LMH based estimates of the local magnetic moment on Fe sites are rather large compared with the one experimental datum available [58]. The experimental value for the local magnetic moment of Pt in this concentration is not available. The experimentally estimated average magnetic moment is significantly lower than that of the calculated values using both local as well as non-local exchange correlations. However, all the available theoretical estimates by different groups [55, 58] are significantly higher, just like ours, compared to the experimental estimate quoted by Osterloh [58]. The experimental result may be interpreted assuming the magnetic moment at the Fe and Pt sites to be arranged antiparallely, giving rise to a ferrimagnetic ground state. However, we were unable to show any theoretical evidence for this and our calculations do predict a stable ferromagnetic alignment as pointed out by Osterloh *et al* [58]. As in the case of Fe_3Pt, the slight difference between the values obtained by Podgorny [55] and by us is again due to the difference in the calculational details. In addition to using the frozen core approximation and neglect of f states in the Pt site, Podgorny has assumed the cubic crystal structure for FePt in a $L1_0$ structure while in reality it is tetragonal. In our calculations, we have assumed the experimentally observed tetragonal structure. The local magnetic moments obtained by Osterloh *et al* [58] using the augmented spherical wave method are higher than ours as well as the calculations by Podgorny [55].

The experimental ground state ordered magnetic phase $FePt_3$ is antiferromagnetic. We have carried out calculations on this alloy both in the ferromagnetic as well as the antiferromagnetic structures. We have found the total energy in the case of the antiferromagnetic structure is indeed lower than that of the ferromagnetic structure. In the ferromagnetic calculation, the local as well as the average magnetic moment obtained by Podgorny [55] using a VWN exchange–correlation potential with theoretical estimates of lattice parameters is in close agreement with our corresponding value. The calculated local magnetic moment on Fe sites by Tohyama *et al* [59] using an empirical tight binding model is

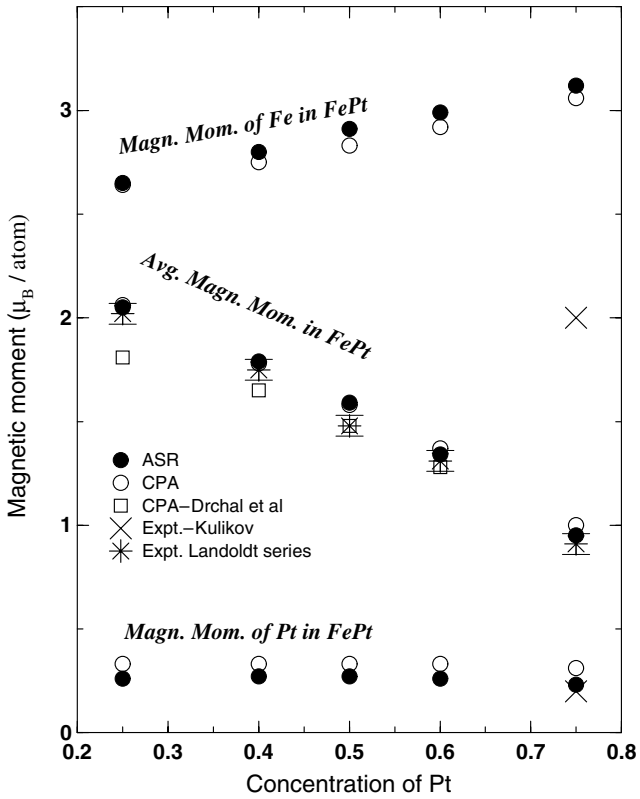

Figure 1. Magnetic moments in disordered Fe–Pt alloy systems using two different configuration averaging methods, namely augmented space recursion (ASR) and coherent potential approximation (CPA), compared to available experimental values given in the Landoldt series [62].

significantly higher than both ours and that of Podgorny [55]. Our calculated magnetic moment on the Fe site for the antiferromagnetic structure using a PW non-local exchange correlation with theoretically estimated lattice parameters is in close agreement with the experimental value [60]. This is the one case where LMH underestimates the staggered magnetization.

3.2.2. Disordered alloys. In figure 1, we compare our calculated disordered magnetic moments using augmented space recursion with the available experimental values taken from the Landoldt series [62] as well as with CPA calculations. The average magnetic moments agree quite well with the corresponding experimental values at all concentrations. The numerical values of local as well as average magnetic moments calculated using LMTO-CPA are in agreement with those obtained using the ASR. This shows that the single-site approximation like CPA works well for the Fe–Pt disordered alloys. The average magnetic moments obtained by Drchal *et al* [63] using CPA matches well for most concentrations though they deviate a bit at low concentrations of Pt. Our calculations use charge neutral spheres to reduce the effect of the Madelung constant whereas Drchal *et al* [63] have used equal Weigner–Seitz radii of both constituents and the effect of the Madelung constant due to charge transfer was taken into account using the screened impurity model [63]. The local moment on the Fe sites increases towards the isolated Fe moment as the concentration of Pt increases. This is an indication of

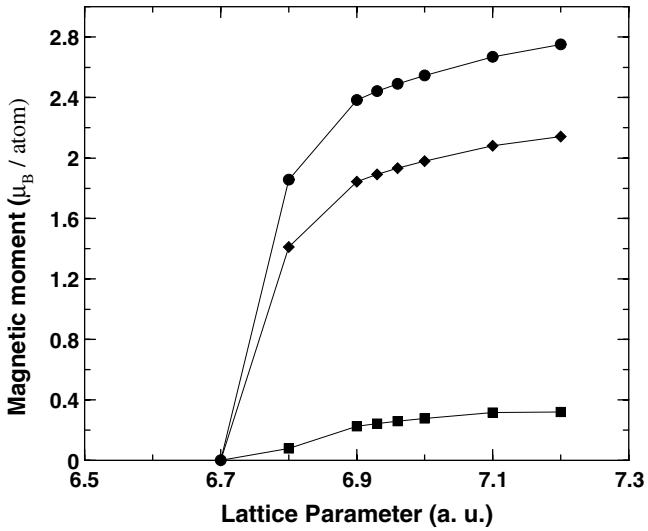

Figure 2. Magnetic moments as a function of lattice parameters for 25% concentration of Pt in a disordered Fe–Pt alloy. Circles, squares and diamonds denote local magnetic moment on Fe site, local magnetic moment on Pt site and average magnetic moment, respectively.

the fact that local environmental effects are unimportant and consequently the CPA and ASR results agree closely.

At 25% concentration of Pt there is the invar effect which shows anomalies in the thermal expansion. We have observed two minima of total energy, one with a high moment and a large lattice constant (6.93 au) and the other with a zero moment and small lattice constant (6.71 au). The total energy difference between the magnetic and non-magnetic states is 2.4 mRyd/atom, which is higher than the calculations by Drchal *et al* (0.7 mRyd/atom) and lower than that of Staunton *et al* (15.7 mRyd/atom). In figure 2, we show the behaviour of the magnetic moment as a function of the lattice parameter which shows the non-magnetic to ferromagnetic transition at 6.71 au. Our calculated average as well as local magnetic moments on Fe and Pt sites corresponding to the theoretically estimated lattice parameter of 6.93 au via total energy minimization on the magnetic state are, respectively, 1.89, 2.44 and 0.24 μ_B.

Table 3 summarizes the known experimental and earlier theoretical results on disordered FePt with 25% Pt. The reported experimental results in this case differ from each other. The localized components of the magnetic moments for Fe ($2.03 \pm 0.02\,\mu_B$) and Pt ($0.34 \pm 0.08\,\mu_B$) were estimated from spin polarized neutron diffraction measurements by Ito *et al* [64], while the magnetization measurements of Caporaletti and Graham [65] indicated moments of 2.75 and 0.45 μ_B for Fe and Pt, respectively. The values of average magnetic moments quoted in the Landoldt series for different experiments are 2.02 and 2.27 μ_B. The theoretical estimates based on different methods also differ from one another. These differences are mainly due to the differences in the computational details chosen in each framework and also in the approximations being used in each method.

For a 75% concentration of Pt our estimate of the magnetic moment on Fe sites is higher than that measured by Kulikov *et al* [60] (which is about 2 μ_B). In order to check the possible short-range order effect, we have checked the variation of total energy as a function of short-range order and found that the total energy decreases as short-range order goes from positive (segregation side) to negative (ordering side), confirming this system as an ordering system. We

Table 3. Various estimates of the local and averaged magnetic moments in Bohr-magnetons for a disordered $Fe_{75}Pt_{25}$ alloy.

Author	Fe	Pt	Average
Expt. [64]	2.03 ± 0.02	0.34 ± 0.08	1.61 ± 0.03
Expt. [65]	2.75	0.45	2.20
Expt. (a) [62]			2.02
Expt. (b) [62]			2.27
LMTO-CPA [63]			1.81
KKR-CPA [66]	2.80	0.23	2.16
LCAO-CPA [67]			2.17
ASR (this work)	2.44	0.24	1.89

have also checked the variation of the magnetic moments as functions of the SRO parameter. We find that both the local and average magnetic moments increase as the SRO parameter goes from the segregating to the ordering side. This is justified by the fact that the magnetic moment of Fe is enhanced when it is surrounded by Pt, as we have seen in the ordered alloys. We therefore conclude that the discrepancy with the experimental data of Kulikov *et al* [60] cannot be due to the short-range ordering effect alone, so probably the other possible factors influencing the experimental results need to be considered.

3.3. Magnetism in Co–Pt alloys

3.3.1. Ordered alloys. Table 4 shows the calculated and experimental magnetic moments for ordered Co–Pt alloys. No experimental result is available for 25% concentration of Pt in the ordered case. The local as well as average magnetic moments obtained by Auluck *et al* [54] using a vBH exchange–correlation potential with the experimental lattice parameter are lower (by 0.30 μ_B for a Co site, 0.01 μ_B for a Pt site and 0.23 μ_B for the average) than our corresponding values, which could be due to differences in computational details as mentioned in the case of Fe–Pt. The local as well as average magnetic moments obtained by Kootte *et al* [68] using the localized spherical wave method using vBH exchange correlation and experimental lattice parameters are in agreement with our corresponding values.

For 50% concentration of Pt, our results agree well with the previous theoretical results [54, 68, 69] within the error bars of the different calculational schemes and are in reasonable agreement with the observed magnetic moments [68] as summarized in table 4.

For 75% concentration of Pt, the calculated local magnetic moments on the Co site and that of the average magnetic moments using possible exchange correlations with both theoretically estimated as well as experimental lattice parameters are on the high side as compared to the experimental estimates [68]. The calculated local moment of Pt using vBH exchange correlation and a theoretically estimated lattice parameter is close to the experimental value [68]. The theoretical estimates for local as well as average magnetic moments by Auluck *et al* [54] and Kootte *et al* [68] for a 50% concentration of Pt are in agreement with our corresponding estimates, as can be seen from table 4. The slight differences seen are again due to differences in the computational details. The local magnetic moments calculated by Tohyama *et al* [59] using the tight binding method are significantly higher than ours as well as experimental estimates which can be seen from table 4. The recent work by Lange *et al* [70] using fully relativistic TB-LMTO with vBH exchange correlation and theoretically estimated lattice parameters report the local as well as the average magnetic moment close to our corresponding values. Their experimental value for the average magnetic moment

Table 4. The local and average magnetic moments of the Co–Pt system in ordered structures with various choices of exchange–correlation functionals.

Concentration of Pt	XC used/expt. ref.	Magnetic moment (μ_B/atom) of					
		With eq. lat. par.			With expt. lat. par.		
		Co	Pt	Average	Co	Pt	Average
0.00 (hex)	vBH (this work)	1.55			1.60		
	VWN (this work)	1.58			1.62		
	LMH (this work)	1.62			1.64		
	PW (this work)	1.67			1.63		
	Expt. Kootte [68]				1.58		
(FCC)	vBH (this work)	1.57			1.62		
	VWN (this work)	1.60			1.64		
	LMH (this work)	1.65			1.67		
	PW (this work)	1.70			1.66		
	Expt. Kootte [68]				1.61		
0.25 ($L1_2$)	vBH (this work)	1.56	0.35	1.26	1.69	0.39	1.37
	VWN (this work)	1.63	0.37	1.32	1.73	0.40	1.40
	LMH (this work)	1.73	0.40	1.40	1.76	0.39	1.42
	PW (this work)	1.80	0.39	1.45	1.74	0.41	1.41
	Auluck *et al* [54]				1.39	0.38	1.14
	Kootte [68]				1.64	0.36	1.32
0.50 ($L1_0$)	vBH (this work)	1.69	0.38	1.03	1.79	0.38	1.09
	VWN (this work)	1.74	0.39	1.07	1.83	0.39	1.11
	LMH (this work)	1.82	0.40	1.11	1.87	0.39	1.13
	PW (this work)	1.91	0.42	1.16	1.83	0.40	1.12
	Auluck *et al* [54]				1.85	0.38	1.12
	Kootte [68]				1.69	0.37	1.03
	Uba [69]				1.60	0.30	
	Expt. Cable [68]				1.70	0.25	0.98
	Expt. van Laar [68]				1.60	0.30	0.95
0.75 ($L1_2$)	vBH (this work)	1.71	0.25	0.62	1.74	0.26	0.64
	VWN (this work)	1.75	0.26	0.63	1.82	0.27	0.65
	LMH (this work)	1.83	0.28	0.67	1.87	0.28	0.68
	PW (this work)	1.95	0.36	0.76	1.82	0.31	0.69
	Auluck *et al* [54]				1.85	0.25	0.65
	Kootte *et al* [68]				1.69	0.27	0.63
	Tohyama *et al* [59]				2.88	0.38	
	Lange *et al* [70]	1.72	0.25	0.62			
	Uba *et al* [69]				1.74	0.24	
	Expt. Menginger [68]				1.64	0.26	0.61
	Expt. Lange *et al* [70]						0.70

matches our corresponding calculated value using non-local exchange–correlation potentials and experimentally estimated lattice parameters. The supercell calculation of Uba *et al* [69] with LMTO using a vBH exchange–correlation potential and experimental lattice parameters agrees well with our corresponding value.

3.3.2. Disordered alloys. In figure 3, we have shown the comparison of local magnetic moments of Co and Pt as well as the average magnetic moment of the disordered Co–Pt

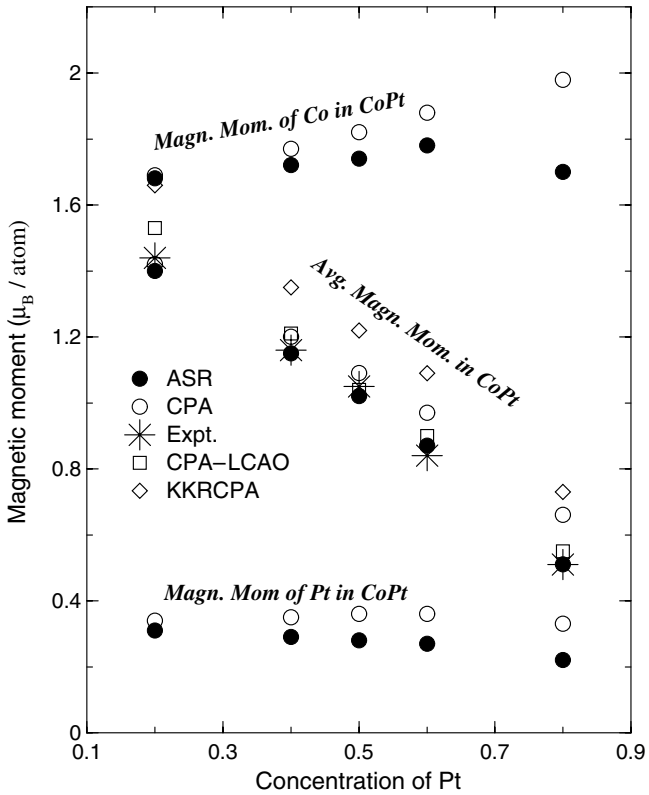

Figure 3. Magnetic moments in disordered Co–Pt alloy systems using two different linearized muffin-tin orbital (LMTO) based configuration averaging methods, namely augmented space recursion (ASR) and coherent potential approximation (CPA) as compared to available experimental values given in the Landoldt series [62]. CPA-LCAO and KKR-CPA denote the coherent potential approximation based linear combination of atomic orbitals method of Koepernik *et al* [67] and the Korringa–Kohn–Rostoker coherent potential approximation method of Ebert *et al* [72], respectively.

system. Calculations have been done both within the ASR and CPA schemes using vBH exchange correlations. The comparison with experimental results for the average magnetic moment taken from the Landoldt series [62] matches well with our calculations. The calculated magnetic moments with the augmented space recursion method are in better agreement with experimental results than that of the coherent potential approximation method. From this figure we can see that the local moment of Co obtained by ASR calculation is almost constant with the increase in concentration of Pt which is the signature of a weak local environmental effect on the Co site. This finding is in agreement with that of Sanchez *et al* [71] who also pointed out the almost constant magnetic moment at the Co site as a function of Pt concentration. The average magnetic moments obtained by Koepernik *et al* [67] using a linear combination of atomic orbitals combined with the coherent potential approximation (LCAO-CPA) method, taking into account both diagonal and off-diagonal disorder effects, show close agreement with our results (except for 20% concentration of Pt where the value obtained by Koepernik *et al* [67] is in better agreement than ours) using augmented space recursion (ASR).

The results obtained by Ebert *et al* [72] using the Korringa–Kohn–Rostoker coherent potential approximation (KKR-CPA) are higher than ours as well as the experimental values. The calculations by Ebert *et al* [72] using KKR-CPA with a single-site approximation were,

though fully relativistic and did not take into account lattice relaxation and off-diagonal disorder effects. Therefore it is not surprising that our calculations show better agreement with experiments. According to the calculation of Shick *et al* [73] using the fully relativistic linearized muffin-tin orbital based coherent potential approximation (LMTO-CPA) method the average and partial magnetic moments of Co and Pt in $Co_{50}Pt_{50}$ are 1.07, 1.79 and 0.35 μ_B, respectively, while the value of Ghosh *et al* [39] using ASR are 1.05, 1.85 and 0.24 μ_B for the same. Our values in this case are 1.05, 1.80 and 0.29. The reason behind the differences seen between the LMTO-CPA of Shick *et al* [73] and ASR is again the same as explained above in connection with KKR-CPA and ASR. Though the calculations by Ghosh *et al* [39] (using a theoretically estimated lattice parameter) and ours (using an experimental lattice parameter) used the same ASR method, ours being charge neutral and self-consistent shows better agreement for local magnetic moments with corresponding charge neutral and self-consistent calculations.

In order to investigate the possible influence of short-range order on disordered magnetic moments, we have performed a complete investigation in terms of the total energy calculations as a function of the short-range order parameter. Like Fe–Pt, Co–Pt also shows a tendency to order. We have also checked the variation of magnetic moments as a function of the SRO parameter and find almost constant local as well as average magnetic moments as the SRO parameter goes from the segregating side to the ordering side, confirming the very small effect of short-range order on the magnetism of the Co–Pt alloy system.

3.4. Magnetism in Ni–Pt alloys

3.4.1. Ordered alloys. In table 5, we show two sets of ordered calculations in Ni–Pt alloys using possible local as well as non local exchange–correlation potentials, one with theoretically calculated lattice constants via the energy minimization procedure and another using experimental lattice parameters.

For 25% concentration of Pt, the calculated local as well as average magnetic moments in ordered Ni–Pt alloys obtained using a vBH local exchange–correlation potential for a theoretically calculated lattice parameter show very good agreement with experimental values [75]. The values obtained by Singh [74] in the same case are higher in comparison to ours and experimental estimates [75]. Singh's [74] calculations seemingly did not include the f states in Pt in the TB-LMTO basis. Our test calculations without including the f states of Pt also show higher values of magnetic moments for this concentration of the Ni–Pt alloy.

For 50% concentration of Pt in a $L1_0$ structure calculated local as well as average magnetic moments using a vBH exchange–correlation potential with the use of an experimental lattice parameter is closest to the experimental estimate [75]. Our calculations with the use of local exchange–correlations and theoretically estimated lattice parameters lead to a non-magnetic ground state which is in agreement with that found in a previous study by Dahmani *et al* [76]. In our calculations we have taken into account the tetragonal distortion as in the case of Fe–Pt and Co–Pt alloys in a $L1_0$ structure.

For 75% concentration of Pt, for a $NiPt_3$ alloy in a $L1_2$ structure there is no experimental result available. For this concentration we have got a higher local magnetic moment of Ni than at the 50% concentration of Pt. This was obtained while using local exchange correlations. In this case if we use non-local exchange correlations then we get the decrease in the local magnetic moment of Ni on going from 50% to 75% concentration of Pt. The average as well as the local magnetic moments on Pt sites show the decreasing tendency using both local as well as non-local exchange correlations with theoretically as well as experimentally estimated lattice constants.

Table 5. The local and average magnetic moments of the Ni–Pt system in ordered structures with various choices of exchange–correlation functionals.

Concentration of Pt	XC used/expt. ref.	Magnetic moment (μ_B/atom) of					
		With eq. lat. par.			With expt. lat. par.		
		Ni	Pt	Average	Ni	Pt	Average
0.00 (FCC)	vBH (this work)	0.61			0.62		
	VWN (this work)	0.62			0.64		
	LMH (this work)	0.64			0.65		
	PW (this work)	0.66			0.64		
	Expt. [57]	0.62					
0.25 ($L1_2$)	vBH (this work)	0.50	0.24	0.43	0.57	0.27	0.49
	VWN (this work)	0.54	0.26	0.47	0.60	0.29	0.52
	LMH (this work)	0.62	0.29	0.53	0.65	0.30	0.56
	PW (this work)	0.71	0.36	0.63	0.63	0.32	0.56
	Singh [74]	0.58	0.27	0.50			
	Expt. Parra *et al* [75]				0.49	0.25	0.43
0.50 ($L1_0$)	vBH (this work)	0.00	0.00	0.00	0.33	0.17	0.25
	VWN (this work)	0.06	0.03	0.05	0.46	0.23	0.34
	LMH (this work)	0.55	0.27	0.41	0.65	0.31	0.48
	PW (this work)	0.72	0.34	0.53	0.63	0.32	0.48
	Singh [74]	0.60	0.27	0.44			
	Expt. Parra *et al*[75]				0.28	0.17	0.22
0.75 ($L1_2$)	vBH (this work)	0.47	0.09	0.18	0.55	0.10	0.21
	VWN (this work)	0.50	0.09	0.20	0.57	0.11	0.22
	LMH (this work)	0.55	0.11	0.22	0.61	0.12	0.24
	PW (this work)	0.65	0.16	0.28	0.58	0.12	0.24
	Singh [74]	0.58	0.10	0.22			

The calculations by Singh [74] using vBH exchange correlations and theoretically estimated lattice parameters show that the local magnetic moment of Ni increases while going from 25% to 50% and decreases while going from 50% to 75% concentration of Pt. The calculations by Singh [74] did not take into account the tetragonal distortion for a 50% concentration of Pt, which means putting the lattice parameters $a = c$, which is not the right ground state structure. For a test we also repeated our calculation without taking into account the tetragonal distortion for a 0% concentration of Pt using vBH local exchange–correlation potentials and theoretically estimated lattice constants and we also observed the same trend that Singh obtained. However, for the calculation taking into account the degrees of freedom for tetragonal distortion we found that the magnetic moments vanish with the use of local exchange–correlation potentials in theoretically estimated lattice parameters.

3.4.2. Disordered alloys. We have plotted the local and average magnetic moments of a disordered Ni–Pt system in figure 4. The comparison of calculated disordered magnetic moments using the augmented space recursion (ASR) method with vBH exchange–correlation potentials and an experimental lattice parameter matches well with experimental values [75] at all concentrations except 55% and 57% of Pt. Our calculations of magnetic moments using the

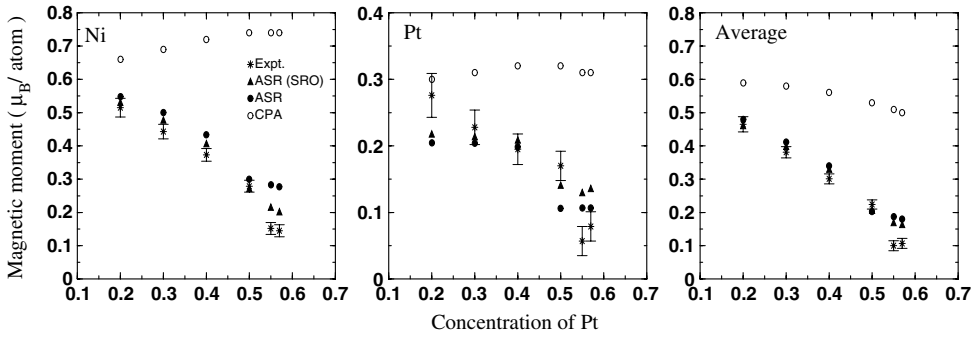

Figure 4. Magnetic moments in disordered Ni–Pt alloy systems using two different configuration averaging methods, namely augmented space recursion (ASR) and coherent potential approximation (CPA) as compared to experimental values given by Parra *et al* [75]. ASR (SRO) denotes the results with a short-range ordering effect using ASR.

coherent potential approximation (CPA) method using a vBH exchange–correlation potential and experimental lattice parameters are very different from the calculations using the ASR method and experimental estimates [75]. Using CPA the local magnetic moments of Ni do not even follow the trend of corresponding experimental estimates. ASR, being capable of going beyond the single-site approximation taking into account lattice relaxation and the off-diagonal disorder effect which is very important in NiPt alloys as was shown in our previous paper [77], provides better agreement with experiment than CPA. Our calculated values for the 55% and 57% concentrations of Pt using the ASR method are on the high side in comparison to the experimental estimates, which leads us to suspect the presence of the short-range ordering effect. We performed calculations incorporating short-range order for all concentrations of Pt in this system and found that the magnetic moments of Ni decreased by an appreciable fraction for the 55% and 57% concentration of Pt. The moment of Pt increases slightly. These give rise to the decrease of average magnetic moment in these concentrations. Calculations incorporating the effect of short-range order agree well with experimental estimates of Parra and Cable [75].

4. Summary and conclusions

To summarize, our study on ordered alloys to investigate the role played by different possible exchange–correlation functionals shows that the choice of exchange–correlation potential has a considerable effect on the values of the equilibrium lattice constants as well as the magnetic moments.

The present study on disordered alloys shows that the single-site approximation based methods work reasonably well for Fe–Pt systems and are in close agreement with our ASR predictions. For the Co–Pt system, the CPA begins to deviate from the ASR. CPA based calculations show a slight increase in the local magnetic moment of Co with increasing Pt concentration, while the ASR shows almost constant behaviour. This indicates the signature of weak local environmental effects on Co sites.

It is in the Ni–Pt alloy that CPA shows the largest deviation from the ASR. The CPA estimates of the magnetic moments are quite different from the experimental values. It predicts an increase of the local magnetic moment on Ni with increasing Pt concentration, whereas experimentally the reverse behaviour is observed. In the absence of local environment effects,

an increase of Pt concentration in Ni–Pt should lead to an increase in the local Ni moment, since isolated clusters of Ni in Pt become more probable. This leads to narrowing of the local density of states on Ni and consequently, according to the Stoner picture, an increase in the local Ni moment. Finally in the dilute limit, this local moment should approach the moment of an isolated Ni atom. This behaviour is certainly seen in Fe–Pt alloys. However, the fragile moment on Ni seems to need at least 50% Ni atoms in its nearest-neighbour environment, otherwise it loses its local moment. This is indeed what one sees in experiment and is a strong indicator of a large local environmental effect in Ni–Pt. The CPA predicts an increase of the local magnetic moment on Ni with increasing Pt concentration. This is expected, since the CPA does not take into account the effect of the local environment. The ASR, however, predicts the correct trend with increasing Pt concentration. The estimates of the actual value of the local magnetic moments are also much better.

Our total energy calculation as a function of short-range order confirms the ordering tendency in these systems. The calculation of magnetic moments as a function of short-range order shows that its effect is small on the magnetism in Fe–Pt and Co–Pt disordered alloys but significant on the magnetism of disordered Ni–Pt.

Finally, the numerical details of calculations, convergence with the number of k points in the Brillouin zone integrations, choice of atomic sphere radii, proper convergences in the CPA and the ASR and the proper choice of the minimal basis set in the TB-LMTO: all of these affect the actual values of the estimated magnetic moments.

Appendix

Details of the methodology of augmented space recursion has been presented in earlier papers referred to in the text. Here we shall quote the key results of TBLMTO-ASR generalized to take into account the short-range ordering effect. The augmented space Hamiltonian including short-range order can be written as

$$\begin{aligned}\hat{H} = {} & H_1 + H_2 \sum_R P_R \otimes P_\downarrow^R + H_3 \sum_R P_R \otimes (T_{\downarrow\uparrow}^R + T_{\uparrow\downarrow}^R) \\ & + H_4 \sum_R \sum_{R'} T_{RR'} \otimes \mathcal{I} + \alpha H_2 \sum_{R''} P_{R''} \otimes P_\downarrow^1 \otimes (P_\uparrow^{R''} - P_\downarrow^{R''}) \\ & + H_5 \sum_{R''} P_{R''} \otimes P_\downarrow^1 \otimes (T_{\uparrow\downarrow}^{R''} + T_{\downarrow\uparrow}^{R''}) \\ & + H_6 \sum_{R''} P_{R''} \otimes P_\downarrow^1 \otimes (T_{\uparrow\downarrow}^{R''} + T_{\downarrow\uparrow}^{R''}) \\ & + \alpha H_2 \sum_{R''} P_{R''} \otimes (T_{\uparrow\downarrow}^1 + T_{\downarrow\uparrow}^1) \otimes (P_\uparrow^{R''} - P_\downarrow^{R''}) \\ & + H_7 \sum_{R''} P_{R''} \otimes (T_{\uparrow\downarrow}^1 + T_{\downarrow\uparrow}^1) \otimes (T_{\uparrow\downarrow}^{R''} + T_{\downarrow\uparrow}^{R''}) \end{aligned} \tag{A.1}$$

where R'' belong to the set of nearest neighbours of the site labelled R, at which the local density of states will be calculated. P's and T's are the projection and transfer operators either in the space spanned by the tight-binding basis $\{|R\rangle\}$ or the configuration space associated with the sites R spanned by $\{|\uparrow_R\rangle, |\downarrow_R\rangle\}$ as described in [49].

$$|\uparrow_R\rangle = \sqrt{x}|A_R\rangle + \sqrt{y}|B_R\rangle \qquad |\downarrow_R\rangle = \sqrt{y}|A_R\rangle - \sqrt{x}|B_R\rangle.$$

The different terms of the Hamiltonian are given below.

$$\begin{aligned}
H_1 &= A(C/\Delta)\Delta_\lambda - (EA(1/\Delta)\Delta_\lambda - 1)\\
H_2 &= B(C/\Delta)\Delta_\lambda - EB(1/\Delta)\Delta_\lambda\\
H_3 &= F(C/\Delta)\Delta_\lambda - EF(1/\Delta)\Delta_\lambda\\
H_4 &= (\Delta_\lambda)^{-1/2} S_{RR'}(\Delta_\lambda)^{-1/2}\\
H_5 &= F(C/\Delta)\Delta_\lambda\left[\sqrt{(1-\alpha)x(x+\alpha y)} + \sqrt{(1-\alpha)y(y+\alpha x)} - 1\right]\\
H_6 &= F(C/\Delta)\Delta_\lambda\left[y\sqrt{(1-\alpha)(x+\alpha y)/x} + x\sqrt{(1-\alpha)(y+\alpha x)/y} - 1\right]\\
H_7 &= F(C\Delta)\Delta_\lambda\left[\sqrt{(1-\alpha)y(x+\alpha y)} - \sqrt{(1-\alpha)x(y+\alpha x)}\right]
\end{aligned} \tag{A.2}$$

where

$$\begin{aligned}
A(Z) &= xZ_A + yZ_B\\
B(Z) &= (y-x)(Z_A - Z_B)\\
F(Z) &= \sqrt{xy}(Z_A - Z_B)
\end{aligned}$$

α is the nearest-neighbour Warren–Cowley parameter described earlier. λ labels the constituents A or B in the case of a binary AB alloy. C and Δ are the potential parameters describing the atomic scattering properties of the constituents and S is the screened structure constant describing the underlying lattice which is face-centred cubic (FCC) in the present case. For convenience, all the angular momentum labels have been suppressed, with the understanding that all potential parameters are 9×9 matrices (for a spd minimal basis set). We note that in the absence of short-range order ($\alpha = 0$), the terms H_5 to H_7 disappear and the Hamiltonian reduces to the standard one described earlier [49].

References

[1] Cadeville M C and Morán-López J L 1987 *Phys. Rep.* **153** 331
[2] Mirebeau L, Cadeville M C, Parette G and Campbell I A 1982 *J. Phys. F: Met. Phys.* **12** 25
[3] Pierron-Bohnes V, Cadeville M C and Parette G 1985 *J. Phys. F: Met. Phys.* **15** 1441
[4] Mirebeau I, Hennion M and Parette G 1985 *Phys. Rev. Lett.* **53** 687
[5] Pierron-Bohnes V, Cadeville M C and Gautier F 1983 *J. Phys. F: Met. Phys.* **13** 1689
[6] Sato H, Arrott A and Kikuchi R 1959 *J. Phys. Chem. Solids* **10** 19
[7] Swalin R A 1962 *Thermodynamics of Solids* (New York: Wiley)
[8] Vonsovskii S V 1974 *Magnetism* (New York: Wiley)
[9] Bieber A, Gautier F, Treglia G and Ducastelle F 1981 *Solid State Commun.* **39** 149
[10] Bieber A and Gautier F 1981 *Solid State Commun.* **38** 1219
[11] Bieber A and Gautier F 1986 *J. Magn. Magn. Mater.* **54–57** 967
[12] Hennion M 1983 *J. Phys. F: Met. Phys.* **13** 2351
[13] Jaccarino V and Walker J L 1965 *Phys. Rev.* **15** 258
[14] Marshall W 1968 *J. Phys. C: Solid State Phys.* **1** 88
[15] Hicks T J 1970 *Phys. Lett.* A **32** 410
[16] Hasegawa H and Kanamori J 1971 *J. Phys. Soc. Japan* **31** 382
[17] Buttler W H 1973 *Phys. Rev.* B **8** 4499
[18] Jo T and Miwa H 1976 *J. Phys. Soc. Japan* **40** 706
[19] Jo T 1976 *J. Phys. Soc. Japan* **40** 715
[20] Hasegawa H 1979 *J. Phys. Soc. Japan* **46** 1504
[21] Hamada N 1979 *J. Phys. Soc. Japan* **46** 1759
[22] Kakehashi Y 1982 *J. Phys. Soc. Japan* **51** 94
[23] Uba S *et al* 1998 *Phys. Rev.* B **57** 1534
Geerts W *et al* 1994 *Phys. Rev.* B **50** 12581
Weller D, Harp G R, Farrow R F C, Cebollada A and Sticht J 1994 *Phys. Rev. Lett.* **72** 2097

[24] Saha T, Dasgupta I and Mookerjee A 1996 *J. Phys.: Condens. Matter* **8** 1979
[25] Mookerjee A 1973 *J. Phys. C: Solid State Phys.* **6** L205
[26] Haydock R, Heine V and Kelly M J 1972 *J. Phys. C: Solid State Phys.* **5** 2845
[27] Haydock R 1988 *Solid State Physics* vol 35 (New York: Academic)
[28] Chakrabarti A and Mookerjee A 2001 *J. Phys.: Condens. Matter* **13** 10149
[29] Saha T and Mookerjee A 1996 *J. Phys.: Condens. Matter* **8** 2915
[30] Lu Z W, Laks D B, Wei S H and Zunger A 1994 *Phys. Rev.* B **50** 6642
[31] Staunton J B, Johnson D D and Pinski F J 1994 *Phys. Rev.* B **50** 1450
[32] Johnson D D, Staunton J B and Pinski F J 1994 *Phys. Rev.* B **50** 1473
[33] Borici-Kuqo M, Monnier R and Drchal V 1998 *Phys. Rev.* B **58** 8355
[34] Wolverton C, Ozolins V and Zunger A 1998 *Phys. Rev.* B **57** 4332
[35] Abrikosov I A, Niklasson A M N, Simak S I and Johansson B 1996 *Phys. Rev. Lett.* **76** 4203
[36] Cowley J M 1950 *J. Appl. Phys.* **21** 24
[37] Mookerjee A and Prasad R 1993 *Phys. Rev.* B **48** 17724
[38] Saha T, Dasgupta I and Mookerjee A 1994 *Phys. Rev.* B **50** 13267
[39] Ghosh S, Chaudhuri C B, Sanyal B and Mookerjee A 2001 *J. Magn. Magn. Mater.* **234** 100
[40] von Barth U and Hedin L 1972 *J. Phys. C: Solid State Phys.* **5** 1629
[41] Vosko S H, Wilk L and Nusair M 1980 *Can. J. Phys.* **58** 1200
[42] Langreth D C and Mehl M J 1981 *Phys. Rev. Lett.* **47** 446
[43] Perdew J P and Wang Y 1986 *Phys. Rev.* B **33** 8800
[44] Andersen O K and Jepsen O 1984 *Phys. Rev. Lett.* **53** 2581
[45] Andersen O K, Jepsen O and Šob M 1987 *Electronic Band Structure and its Applications* (*Springer Lecture Notes in Physics* vol 283) ed M Yussouff (Berlin: Springer) p 1
[46] Andersen O K, Jepson O and Krier G 1994 *Lectures on Methods of Electronic Structure Calculations* ed V Kumar, O K Andersen and A Mookerjee (Singapore: World Scientific)
[47] Das G P 2003 Electronic structure of alloys, surfaces and clusters *Advances in Condensed Matter Science* vol 4, ed A Mookerjee and D D Sharma (London: Taylor and Francis)
[48] Sanyal B, Biswas P P, Mookerjee A, Das G P, Salunke H and Bhattacharya A K 1998 *J. Phys.: Condens. Matter* **10** 5767
[49] Biswas P P, Sanyal B, Fakhruddin M, Halder A, Mookerjee A and Ahmed M 1995 *J. Phys.: Condens. Matter* **7** 8569
[50] Kudrnovský J and Drchal V 1990 *Phys. Rev.* B **41** 7515
[51] Ghosh S, Das N and Mookerjee A 1999 *J. Phys.: Condens. Matter* **9** 10701
[52] Ghosh S D 2000 *PhD Thesis* Jadavpur University
[53] Pearson W B 1964 *A Handbook of Lattice Spacings and Structures of Metals and Alloys* (Oxford: Pergamon) pp 1958–67
[54] Kashyap A, Garg K B, Solanki A K, Nautiyal T and Auluck S 1999 *Phys. Rev.* B **60** 2262
[55] Podgórny M 1991 *Phys. Rev.* B **43** 11300
Podgórny M 1992 *Phys. Rev.* B **46** 6293
[56] Pisanty A, Amador C, Ruiz Y and de la Vega M 1990 *Z. Phys.* B **80** 237
[57] Lide D R 2000 *Hand Book of Chemistry and Physics* 81st edn, pp 12–119
[58] Osterloh I, Oppeneer P N, Sticht J and Kubler J 1994 *J. Phys.: Condens. Matter* **6** 285
[59] Tohyama T, Ohta Y and Shimizu M 1989 *J. Phys.: Condens. Matter* **1** 1789
[60] Kulikov N I, Kulatov E T and Yakhimovich S I 1985 *J. Phys. F: Met. Phys.* **15** 1127
[61] Uhl M, Sandratskii L M and Kubler J 1994 *Phys. Rev.* B **50** 291
[62] Wijn H P J and Landolt–Bornstein (ed) 1986 *Magnetic Properties of Metals 3d, 4d and 5d Elements, Alloys and Compounds* Part a (*Landolt-Bornstein New Series,* Group III, vol 19) (Berlin: Springer)
[63] Hayn R and Drchal V 1998 *Phys. Rev.* B **58** 4341
[64] Ito Y, Sasaki T and Mizoguchi T 1974 *Solid State Commun.* **15** 807
[65] Caporaletti O and Graham G M 1980 *J. Magn. Magn. Mater.* **22** 25
[66] Major Z S, Dugdale S, Jarlborg B, Bruno E, Ginatempo B, Staunton J B and Poulter J 2003 *J. Phys.: Condens. Matter* **15** 3619
[67] Koepernik K, Velický B, Hayn R and Eschrig H 1997 *Phys. Rev.* B **55** 5717
[68] Kootte A, Haas C and de Groot R A 1991 *J. Phys.: Condens. Matter* **3** 1133
[69] Uba L, Uba S, Antonov V N, Yaresko A N and Gontarz R 2001 *Phys. Rev.* B **64** 125105
[70] Lange R J, Lee S J, Lynch D W, Canfield P C, Harmon B N and Zollner S 1998 *Phys. Rev.* B **58** 351
[71] Sanchez J M, Morán-López J L, Leroux C and Cadeville M C 1989 *J. Phys.: Condens. Matter* **1** 491
[72] Ebert H, Drittler B and Akai H 1992 *J. Magn. Magn. Mater.* **104–107** 733

[73] Shick A B, Drchal V, Kudrnovský J and Weinberger P 1996 *Phys. Rev.* B **54** 1610
[74] Singh P P 2003 *J. Magn. Magn. Mater.* **261** 347
[75] Parra R E and Cable J W 1980 *Phys. Rev.* B **21** 5494
[76] Dahmani C E, Cadeville M C, Sanchez J M and Morán-López J L 1985 *Phys. Rev. Lett.* **55** 1028
[77] Paudyal D, Saha-Dasgupta T and Mookerjee A 2003 *J. Phys.: Condens. Matter* **15** 1029